Optical Pulse-Drive for the Pulse-Driven AC Josephson Voltage Standard

Oliver Kieler ⓘ, Bjørnar Karlsen ⓘ, Per Alfred Ohlckers ⓘ, Eivind Bardalen ⓘ, Muhammad Nadeem Akram ⓘ, Ralf Behr ⓘ, Jane Ireland ⓘ, Jonathan Williams, Helge Malmbekk ⓘ, Luis Palafox ⓘ, and Ruediger Wendisch

Abstract—We developed an optical pulse-drive for the operation of the Josephson Arbitrary Waveform Synthesizer (JAWS) using a fast photodiode (PD) operated at 4 K, close to the JAWS chip. The optical pulses are transmitted to the PD by an easily removable optical fiber attached to it. A bare-lensed PD is mounted by flip-chip technique to a custom-made silicon-carrier chip. This carrier chip is equipped with coplanar waveguides to transmit the electrical pulses from the PD to the JAWS chip mounted on a separate printed circuit board (PCB). The main components of this optical setup are a laser source, a high-speed Mach–Zehnder modulator, and the modulator driver. The waveform pattern is supplied by a commercial pulse pattern generator providing up to 15 GHz electrical return-to-zero (RTZ)-pulses. Unipolar sinusoidal waveforms were synthesized. Using a JAWS array with 3000 junctions, an effective output voltage of 6.6 mV root mean square (RMS) at the maximum available clock-frequency of 15 GHz was achieved. Higher harmonics were suppressed by more than 90 dBc at laser-bias operation margins of more than 1 mA.

Index Terms—AC Josephson voltage standard, Josephson arbitrary waveform synthesizer, SNS Josephson junction, sigma-delta modulation, optical pulse-drive, flip-chip technology.

I. INTRODUCTION

AFTER many years since the first realization of a pulse-driven AC Josephson voltage standard [1], recent developments in increasing the effective output voltage to 1 V root mean square (RMS) or even more [2]–[5] show that the use of a pulse-driven Josephson voltage standard is an important approach for voltage metrology. This AC Josephson voltage standard is often called "Josephson Arbitrary Waveform Synthesizer" (JAWS) and it is already used in several NMIs for metrology applications [6]–[15]. For the application in JAWS, the Josephson junctions are operated by short current pulses to

directly transfer flux quanta. According to the Josephson equation, a time-dependent voltage, which is quantized at all times, is generated. The signal-voltage and frequency are well defined by these two basic equations:

$$V_{signal} = A_{\Sigma\Delta} \cdot n \cdot m \cdot \Phi_0 \cdot f_{clock} \qquad (1)$$

$$f_{signal} = T_{\Sigma\Delta} \cdot f_{clock} / L_{\Sigma\Delta} \qquad (2)$$

The output voltage V_{signal} is the product of the Shapiro-step number n (typical: $n = 1$), the number of junctions in the series array m, the flux quanta $\Phi_0 = h/2e$ (h is the Planck constant and e the elementary charge), the sigma-delta code amplitude $A_{\Sigma\Delta}$ ($0 < A_{\Sigma\Delta} < 1$) and the clock-frequency f_{clock}. The maximum pulse-repetition frequency $f_p(t)$ used for our JAWS is 15 GHz, limited by the maximum clock frequency f_{clock} of commercially available pulse pattern generator (PPG). $A_{\Sigma\Delta}$ is a real number ($0 < A_{\Sigma\Delta} < 1$), but well defined. Since the numbers ($A_{\Sigma\Delta}$, n, m) are known, Φ_0 is determined by natural constants and f is very well defined, the JAWS delivers quantized arbitrary waveforms. The signal frequency f_{signal} is determined by the simple equation (2): the number of periods in the code $T_{\Sigma\Delta}$, the clock frequency f_{clock} of the PPG and the length of the waveform bit pattern $L_{\Sigma\Delta}$.

This fundamental approach enables the generation of quantized arbitrary waveforms with excellent spectral purity with low noise and no drift.

The use of an optical drive with photodiodes (PDs) operated at 4 K close to the JAWS chip could improve the JAWS in several ways:

1) Some years ago, Urano et al. [16] presented a JAWS system with optical drive. Our approach, using small bare PDs on a custom-made carrier, could provide an alternative way for parallel operation of several arrays that is easier and more cost efficient, because one optical channel can be split into several channels and each can operate one JAWS array. Therefore, output voltages could be increased to the range of 10 V RMS, which is desired for covering the whole voltage range for applications in DC/AC voltage metrology.

2) The use of optical fibers instead of high-frequency coaxial cables will reduce the thermal load to the system, which is an important aspect for operating JAWS systems in closed-cycle pulse-tube cryocoolers.

3) The optical drive also removes the coupling noise introduced by the PPG, which is important when extending the

Fig. 1.   Block diagram of a JAWS system with optical pulse-drive.

Fig. 2.   Photograph showing the JAWS chip (left) and PDCC chip (right) connected. The optical fiber (white) is attached by glass tube guide to the PD mounted by flip-chip to the PDCC chip.

JAWS to higher signal frequencies above 1 MHz. Moreover, crosstalk between several high-frequency coaxial cables for transferring the pulses, is avoided by an optical drive.

4) Establishing a setup, where the PDs are very close to the JAWS chip significantly reduces the distortion and attenuation of the pulses, thus increasing the operating margins.

Pioneering work was done realizing an optical setup for JAWS [16], [17]. Here, only a small number of junctions (fewer than 500) and lower clock frequencies (up to 10 GHz) were used. As a consequence, the maximum effective output voltage was limited to well below 1 mV RMS.

As part of a collaboration between Justervesenet, University of South-Eastern Norway (USN), NPL and PTB, the development of an optical drive for a JAWS system was also begun [18]–[23].

This paper describes the combination of the newly developed optical pulse-drive system, including the optimized assembly for PD operation at 4 K. For this proof-of-principle experiment just a single JAWS array was used and first results will be presented.

II. SETUP

SNS-type Josephson junctions (S . . . superconductor, N . . . normal conductor) with Nb_xSi_{1-x} [24], [25] as the normal-metal barrier material are used for the realization of several JAWS systems at PTB. The JAWS circuit design is based on a coplanar waveguide (CPW) high-frequency transmission line with series arrays of Josephson junctions embedded in the central conductor, similar to the designs used at NIST [1] and AIST [16]. For the PTB 1.5 V RMS JAWS setup [26], the electrical pulses are delivered by a Sympuls BPG30G-TERx8[1] ternary PPG with a data rate of up to 30 Gbit/s. The electrical pulses are transmitted by a length of about 1.5 m HF coaxial cable from the PPG output to the cryoprobe head. Inside the cryoprobe a 1.2 m semi-rigid HF coaxial cable transfers the pulses to the printed circtuit board (PCB)-carrier at the LHe temperature of 4 K, where the JAWS chip is mounted. One channel of this setup was used for the experiment described here.

This electrical pulse transmission is replaced now by an optical pulse-drive, shown schematically in Fig. 1. The pulse pattern is provided by the PPG (Sympuls, BPG-30G-TERx8) and electrically transferred to the RF Modulator Driver iXblue DR-DG-20-MO (RF-MD), which works as an amplifier for the electrical pulses. This RF-MD is biased at $V_{bias-RF} = 12$ V, $V_{amp-RF} = 0.3$–0.8 V, $V_{xp-RF} = 0.7$–0.8 V and provides a flat gain up

to 10 GHz with a maximum output voltage of 8 V PP. The amplified pulses are transferred electrically to the Mach-Zehnder Modulator iXblue MX1300-LN-20 (MZM). The MZM was an $LiNbO_3$ based intensity modulator designed for 1310 nm lasers operated with a bias voltage of $V_{bias-MZM} = 9.2$–10.2 V. The electro-optical bandwidth is 20 GHz and the electrical and optical properties are well suited for our application. The 1310 nm Fabry-Perot Laser Thorlabs FPL-1053 (FPL) output is coupled to the MZM. The O-band FPL delivers an adjustable maximum optical power of 130 mW, which should be sufficient to operate the PD. From the MZM the optical pulse pattern is guided to the cryoprobe by a 1 m FC/APC to FC/PC optical fiber (angled to flat patch cable) and a 2 m FC/PC to FC/PC fiber extension. A high performance InGaAs PD with an integrated lens (Albis PD20X1) [27] is selected to ensure an output current of up to 7 mA [22] at the operation temperature of 4 K ($V_{bias-PD} = 5$ V). This bottom illuminated PD was optimized for high data rate of at least 28 Gbit/s and offers excellent dynamic response in the wavelength range between 1260 nm and 1620 nm at 300 K. The upper limit at 4 K is about 1510 nm due to the band gap increase at cryogenic temperatures as described in [21]. Providing a relatively large lens diameter of 100 μm, it is easy to implement it to the setup for a robust and reliable operation. Detailed optimizations and investigations of the high-speed performance at room-temperature and 4 K were performed [21], [22] and the optical pulse setup is described [23]. Finally, the PD produces the electrical pulses, which are transferred over a comparable short distance of about 4 cm from the custom-made silicon-based PD-chip-carrier (PDCC) to the JAWS chip (see Fig. 2), both mounted on separate PCB carriers. The PD and the JAWS array are directly coupled. The JAWS chip contains two separate identical JAWS arrays, but only one is used in this paper. Therefore, the lower uncovered SMA connector at the JAWS PCB shown in Fig. 2, is not used. For operation of the different components of the optical setup, the above mentioned six adjustable DC bias supply-voltages are used. A PPG pulse amplitude of 500 mV PP was used to drive the RF-MD. All components of the setup are matched to a 50 Ω impedance.

For electrical and/or optical operation a cryoprobe was constructed, equipped with a semi-rigid HF-cable and a pair of optical fibers (1.5 m FC/PC to 1.8 mm ferrule) to directly transmit the laser pulses to the PD. The fiber input uses an FC/PC connector and is connected to a single mode FC/PC to ferrule fiber inside of the cryoprobe.

The tiny PDs (350 μm $\times$ 350 μm) are illuminated through the lens on the back of the diode and are mounted by a sophis-

ticated flip-chip technology to the PDCC chip [21], [22]. A big advantage for practical use is that the optical fiber, connected via a glass tube glued to the PDCC chip, is removable. This tube is precisely aligned to the PD on-chip to ensure high-efficiency of the illumination. The flip-chip technique was established and performed at USN/JV in cooperation with NPL and PTB. The PDCC chip layout includes the contact pads for the PD, an alignment marker system for the flip-chip procedure of the PD and the alignment of the glass tube. DC-bias lines provide the bias voltage for the PD. The electrical pulses generated by the PD are transmitted by CPW high-frequency transmission lines with an impedance of 50 Ω. The width tapered CPW on the PDCC chip is wire bonded to a PCB-chip carrier, which carries the signals to edge launchers for 2.92 mm connectors.

The PDCC is fabricated at the clean-room facility at PTB using Nb for the DC/HF-lines and AuPd for the alignment markers and contact pads (PD and wire bond pads). An additional SiO_2 layer is deposited by PECVD to effectively protect the sensitive on-chip dc-block capacitors against electrical damage during operation. In particular, the post-clean room attachment of the PD and the gluing of the glass-tube introduces some particle contamination. This PDCC chip is then glued to a specially designed PCB-chip carrier (RO3006 material from Roger Corp.) containing Au-plated 1 oz. Cu-lines with tapered 50 Ω CPW lines to attach K-type PCB-edge connector directly to it. The JAWS PCB chip-carrier (Roger 3006) is connected at this point via an adapter. Both chips, JAWS and PDCC are connected by Al or Au wire bonds to the PCB carriers.

III. MEASUREMENTS

For the measurements presented in this paper, a single JAWS array with 3000 Josephson junctions was selected. The array was characterized by electrical pulses first. The basic parameters are the critical current of 2.8 mA and the characteristic frequency of $f_c = 4.2$ GHz. At a constant pulse repetition frequency of $f_p = 4.2$ GHz the 1st Shapiro step (SS) with a maximum width of 1.8 mA can be generated with optimized pulse amplitude. At 10 GHz this step is still 1.4 mA wide. Synthesizing a sinusoidal waveform with electrical pulses only, pure spectra can be observed up to a sigma-delta code amplitude of $A_{\Sigma\Delta} = 0.9$ at a clock-frequency of $f_{clock} = 14$ GHz. This corresponds to a bipolar output voltage of $V = 55$ mV RMS with current operation margins of about 0.7 mA and a spectral purity of about 112 dBc spurious-free-dynamic-range (SFDR).

Fig. 3 shows three current-voltage characteristics (IVC) for optical pulses applied with constant f_p using a simple 2-bit alternating pulse pattern "10". The IVCs are shifted in the x-axis depending on the laser bias-voltage. Three different pulse repetition frequencies $f_p = f_{clock}/2 = 2.5/5.0/7.5$ GHz were realized ($f_{clock-max} = 15$ GHz). For each frequency the laser bias-voltage (i.e., the pulse amplitude) was adjusted for the maximum width of the Shapiro step. We measured a step width of about 1.9 mA at $f_p = 5$ GHz (with optimized pulse amplitude), which is slightly larger than with electrical pulses. The maximum pulse amplitude available from our optical pulse drive at $f_p = 7.5$ GHz is not sufficient for evolution of the maximum possible Shapiro step width. This will lead to low operating margins or restrict
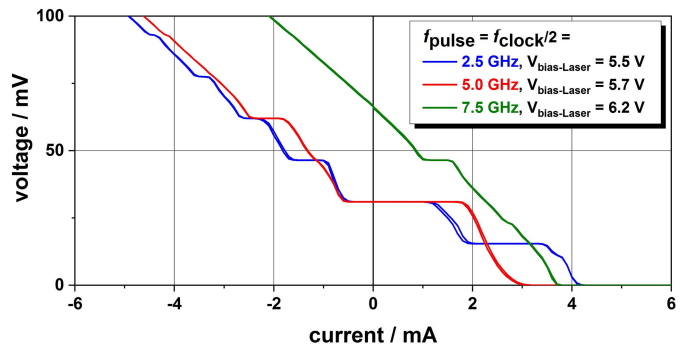

Fig. 3. Current-voltage characteristic under irradiation of optical pulses for 3 different pulse repetition frequencies. The pulse amplitude was adjusted for each frequency to maximize the Shapiro step width.
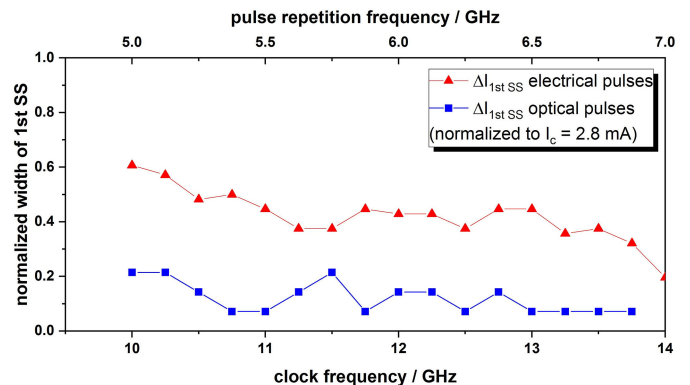

Fig. 4. Normalized Shapiro step width for electrical and optical pulses vs. clock frequency.

the operation to smaller clock frequencies or sigma-delta code amplitudes. Further work is ongoing to overcome this limitation.

Fig. 4 shows the Shapiro step, normalized to the critical current, for electrical and optical pulses in the clock frequency range from 10 GHz to 14 GHz. The same simple bit pattern used in Fig. 3 was applied. The optical pulse amplitude was adjusted in advance to achieve pure spectra at $f_{clock} > 10$ GHz and then was kept constant for all measurements. Although the +1st SS are narrower compared to Fig. 3, they are present at all frequencies, as required for synthesizing pure spectra in pulse-mode operation in JAWS. The width of the optically generated +1st SS is about three times smaller than for the electrical pulses. We note that the power for electrical pulses is reasonably larger, because there is a 16 dB amplifier installed at the PPG output. The Shapiro steps are more or less overlapping in the current axis (not shown). At the highest clock frequencies, the step widths are small (less than 0.3 mA) and the step position is shifted due to the limited pulse power. Again, this is an indicator of possible reduced operation margins at high pulse densities.

Due to the optical setup with just one PD implemented, unipolar waveforms can be synthesized using the 0th SS and +1st SS only. Therefore, the corresponding sigma-delta code, containing the bit-pattern for the desired waveform, was calculated accordingly. A DC-shift was included to ensure, that the minimum AC-voltage is zero. Additionally, only a first-order sigma-delta modulation was applied. Both modifications guarantee that there is no "−1" in the sigma-delta code, avoiding the -1st SS.
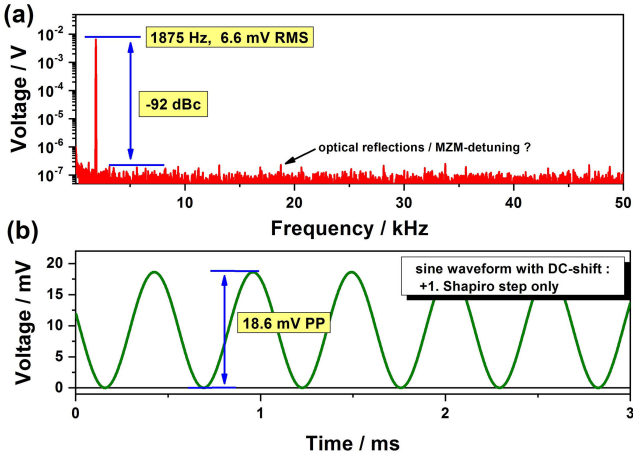
Fig. 5.   (a) Frequency-spectra and (b) time-domain of a unipolar sinusoidal waveform at a signal frequency of 1875 Hz and amplitude of 6.6 mV RMS. A PD operated at 4 K and 15 GHz was used to provide the pulses to the JAWS array with 3000 junctions.

However, due to this unipolar operation the possible maximum output voltage of the JAWS array is reduced by a factor of two.

Fig. 5 shows the frequency spectrum (a) and time-domain signal (b) of a sinusoidal waveform synthesized at the maximal available clock-frequency of $f_{clock} = 15$ GHz. An output voltage of $V = 6.6$ mV RMS at a signal frequency of 1.875 kHz was generated using a sigma-delta code amplitude of $A_{\Sigma\Delta} = 0.2$, where no AC-coupling compensation [28] signal was applied. The time-domain shows the described DC shift of the sine wave – the minimum signal amplitude is at zero voltage. The laser-bias current, determining the pulse amplitude, was the only input parameter for the JAWS array. The Laser-bias operating margins are 1 mA (corresponding to about 300 μW power). The margins are small compared to the total laser power, but sufficient. In this range the signal amplitude and the spectrum were unchanged, which is a clear indication of operation margins. However, no metrological precision measurements were performed to confirm this. No extra dither current was applied to evaluate the overall current operation margins, and only one input parameter was used to operate the JAWS array. The purpose of this paper was to operate the PD as fast as possible for demonstrating the potential of this setup at high speed – regardless of the total range of operation margins. Laser-bias margins of about 1 mA are more than sufficient for many applications already. For lower clock-frequencies the laser-bias operation margins are larger (e.g., at $f_{clock} = 10$ GHz and $A_{\Sigma\Delta} = 0.2$ we determined margins of about 20 mA). The SFDR in Fig. 5(a) is about 92 dBc. Minor distortion tones are visible above the noise floor, which need further investigation. A possible reason is most likely related to MZM detuning and/or optical reflections. Another source of these harmonics could be the wide-range of wave-lengths emitted by the FP-laser. Due to this, the "0" parts of the optical signal cannot be completely extinguished, and noise may arise from this. Distributed Feedback (DFB) and Distributed Bragg Reflector (DBR) lasers provide a narrower range of wave-lengths, but they produce less power at 1310 nm. The connection of the JAWS chip to the PDDC is

far from optimum and might also be the reason for these small distortions.

We also note that for $A_{\Sigma\Delta} > 0.3$ the JAWS is not on quantized operation margins anymore and higher harmonics appear in the frequency spectrum. A detailed analysis of the optical generated pulses and comparison with the electrical pulses from the PPG in [23] was performed. It was discovered that the optical pulses show about 1.5 times larger rise/fall time compared to the electrical pulses at highest clock rates.

Furthermore, the optical pulses do not perfectly return to zero current, when the pulse density is increased. This could directly explain the limitations for higher sigma-delta code amplitudes. However, when investigated with a sampling oscilloscope, the full width at half maximum of the optical pulses was about 80 ps at 4 K [23], which matches electrical pulses that have been successfully used with this JAWS array.

IV. Conclusion

We have tested the performance of an optical pulse-drive setup for JAWS. We used a single JAWS array containing 3000 Josephson junctions with a PD operating at 4 K close to the JAWS chip. The PD was connected by flip-chip technology to a specially manufactured carrier chip. A sophisticated easy-removable connection was developed to attach an optical fiber to the cold PD. This robust solution together with its small footprint offers a cost-efficient operation of several PDs in parallel, together with several JAWS arrays to increase the overall output voltage.

The IVC for constant pulse repetition frequencies at different clock frequencies and pulse amplitudes shows wide +1. Shapiro steps, as a precondition for the generation of arbitrary waveforms by the JAWS in the future. At the highest clock-frequency, the available laser power limited the width of the first Shapiro step that could be measured, which led to reduced operating margins at higher pulse-densities or/and pulse-rates.

We demonstrated a unipolar sinusoidal waveform at 1.875 kHz and 6.6 mV RMS with high spectral purity and wide operation margins, but no metrological precise measurement was performed to confirm the quantum accuracy of the synthesized signal. The PD was operated at the maximum available clock frequency of 15 GHz return-to-zero (RTZ)-pulses.

Further investigations of the pulse quality will be performed in the future. A more powerful laser will be used to overcome the limitations at high pulse repetition frequencies. The connection of the JAWS and the PD carrier chips must be optimized as well. In a next step we will combine two PDs for bipolar operation of a single JAWS array.

REFERENCES

[1] S. P. Benz and C. A. Hamilton, "A pulse-driven programmable Josephson voltage standard," *Appl. Phys. Lett.*, vol. 68, pp. 3171–3173, May 1996.

[2] S.P. Benz *et al.*, "One-volt Josephson arbitrary waveform synthesizer," *IEEE Trans. Appl. Supercond.*, vol. 25, no. 1, Feb. 2015, Art. no. 1300108, doi: 10.1109/TASC.2014.2357760.

[3] O. F. Kieler *et al.*, "Towards a 1 V Josephson arbitrary waveform synthesizer," *IEEE Trans. Appl. Supercond.*, vol. 25, no. 3, Jun. 2015, Art. no. 1400305.

[4] N. E. Flowers-Jacobs, A. E. Fox, P. D. Dresselhaus, R. E. Schwall, and S. P. Benz, "Two-volt Josephson arbitrary waveform synthesizer using wilkinson dividers," *IEEE Trans. Appl. Supercond.*, vol. 26, no. 6, Sep. 2016, Art. no. 1400207.

[5] N. E. Flowers-Jacobs *et al.*, "Three volt pulse-driven Josephson arbitrary waveform synthesizer," in *Proc. CPEM 2018 Dig.*, Paris, France, Jul. 2018, doi: 10.1109/CPEM.2018.8501053.

[6] S. P. Benz, C. J. Burroughs, and P. D. Dresselhaus, "Low harmonic distortion in a Josephson arbitrary waveform synthesizer," *Appl. Phys. Lett.*, vol. 77, pp. 1014–1016, Aug. 2000.

[7] S. P. Benz *et al.*, "An AC Josephson voltage standard for AC-DC transfer standard measurements," *IEEE Trans. Inst. Meas.*, vol. 56, no. 2, pp. 239–243, Apr. 2007.

[8] T. E. Lipe, J. R. Kinard, Y.-H. Tang, S. P. Benz, C. J. Burrroughs, and P. D. Dresselhaus, "Thermal voltage converter calibrations using a quantum AC standard," *Metrologia*, vol. 45, pp. 275–280, May 2008.

[9] E. Houtzager, S. P. Benz, and H. E. van den Brom, "Operating margins for a pulse-driven Josephson arbitrary waveform synthesizer using a ternary bit-stream generator," *IEEE Trans. Inst. Meas.*, vol. 58, no. 4, pp. 775–780, Apr. 2009.

[10] D. Schleussner, O. F. Kieler, R. Behr, J. Kohlmann, and T. Funck, "Investigations using an improved Josephson arbitrary waveform synthesizer (JAWS) system," in *Proc. CPEM 2010 Dig.*, Daejeon, South Korea, Jun. 2010, pp. 177–178.

[11] P. S. Filipski, H. E. van den Brom, and E. Houtzager, "International comparison of quantum AC voltage standards for frequencies up to 100 kHz," *Measurement*, vol. 45, pp. 2218–2225, Mar. 2012.

[12] D. Georgakopoulos, I. Budovsky, S. P. Benz, and G. Gubler, "Josephson arbitrary waveform synthesizer as reference standard for the measurement of the phase of harmonics in distorted signals," in *Proc. CPEM 2018 Dig.*, Paris, France, Jul. 2018, doi: 10.1109/CPEM.2018.8501223.

[13] I. Budovsky, D. Georgakopoulos, and S. P. Benz, "120 V AC voltage measurements using a Josephson arbitrary waveform synthesizer and an inductive voltage divider," in *Proc. CPEM 2018 Dig.*, Paris, France, Jul. 2018, doi: 10.1109/CPEM.2018.8501176.

[14] Y. Chong, M. S. Kim, S. W. Kwon, W. S. Kim, and K. T. Kim, "Application of a pulse-driven AC Josephson voltage standard to ac-dc difference measurement in KRISS," in *Proc. CPEM 2012 Dig.*, Washington, DC, USA, Jul. 2012, doi: 10.1109/CPEM.2012.6250652.

[15] K. Zhou, J. Qu, X. Xu, and Z. Zhou, "Thermal transfer standard calibrations using a pulse-driven AC Josephson voltage standard," in *Proc. CPEM 2018 Dig.*, Paris, France, Jul. 2018, doi: 10.1109/I2MTC.2015.7151328.

[16] C. Urano *et al.*, "Operation of a Josephson arbitrary waveform synthesizer with optical data input," *Supercond. Sci. Technol.*, vol. 22, Oct. 2009, Art. no. 114012.

[17] J. M. Williams *et al.*, "The simulation and measurement of the response of Josephson junctions to optoelectronically generated short pulses," *Supercond. Sci. Technol.*, vol. 17, pp. 815–818, 2004.

[18] J. Ireland *et al.*, "An optoelectronic coupling for pulse-driven Josephson junction arrays," in *Proc. CPEM 2014 Dig.*, Aug. 2014, doi: 10.1109/CPEM.2014.6898290.

[19] J. Ireland *et al.*, "Josephson arbitrary waveform system with optoelectronic drive," in *Ext. Abstract, ISEC-2017: 16th Int. Supercond. Electron. Conf.*, Sorrento, Italy, Jun. 2017, pp. 12–16.

[20] J. Kohlmann, O. Kieler, R. Wendisch, B. Egeling, and R. Behr, "Progress of pulse-driven AC Josephson voltage standards at PTB," in *Proc. EUCAS 2017, 13th Eur. Conf. Appl. Supercond.*, Geneva, Switzerland, Sep. 2017, pp. 17–21.

[21] E. Bardalen, B. Karlsen, H. Malmbekk, O. Kieler, M. N. Akram, and P. Ohlckers, "Packaging and demonstration of optical-fiber-coupled photodiode array for operation at 4 K," *IEEE Trans. Comp. Pack. Manuf. Technol.*, vol. 7, no. 9, pp. 1395–1401, Sep. 2017.

[22] E. Bardalen, B. Karlsen, H. Malmbekk, O. Kieler, M. N. Akram, and P. Ohlckers, "Reliability study of fiber-coupled photodiode module for operation at 4 K," *Microelectron. Rel.*, vol. 81, pp. 362–367, 2018.

[23] B. Karlsen *et al.*, "Pulsation of InGaAs photodiodes in liquid helium for driving Josephson arrays in ac voltage realization," *IEEE Trans. Appl. Supercond.*, to be published.

[24] B. Baek, P. D. Dresselhaus, and S. P. Benz, "Co-sputtered amorphous $Nb_x Si_{1-x}$ barriers for Josephson-junction circuits," *IEEE Trans. Appl. Supercond.*, vol. 16, no. 4, pp. 1966–1970, Dec. 2006.

[25] O. Kieler, R. Behr, D. Schleussner, L. Palafox, and J. Kohlmann, "Precision comparison of sine waveforms with pulse-driven Josephson arrays," *IEEE Trans. Appl. Supercond.*, vol. 23, no. 3, Jun. 2013, Art. no. 1301404.

[26] O. Kieler, R. Behr, R. Wendisch, and J. Kohlmann, "Arrays of stacked SNS Josephson junctions for pulse-driven Josephson voltage standards," in *Proc. EUCAS 2017, 13th Eur. Conf. Appl. Supercond.*, Geneva, Switzerland, Sep. 2017, pp. 17–21.

[27] Albis Optoelectronics, Switzerland, Data Sheet for PD20X1 28 Gb/s photodiode with integrated lens. Available: www.albisopto.com/albis_product/pd20x1/

[28] S. P. Benz, C. J. Burroughs, and P. D. Dresselhaus, "AC coupling technique for Josephson waveform synthesis," *IEEE Trans. Appl. Supercond.*, vol. 11, no. 1, pp. 612–616, Mar. 2001.